Proceedings IRF2018: 6th International Conference Integrity-Reliability-Failure
Lisbon/Portugal 22-26 July 2018. Editors J.F. Silva Gomes and S.A. Meguid
Publ. INEGI/FEUP (2018); ISBN: 978-989-20-8313-1

PAPER REF: 7116

A METHOD FOR MASS BURNING RATE CALCULATION IN FOUR STROKE SPARK IGNITION INTERNAL COMBUSTION ENGINES

Pedro Carvalheira(*)

Dep. Engª Mecânica, Faculdade de Ciências e Tecnologia da Universidade de Coimbra, Coimbra, Portugal
(*) *Email:* pedro.carvalheira@dem.uc.pt

ABSTRACT

This work presents a method for the calculation of mass burning rate in the combustion chamber of four-stroke spark ignition internal combustion engines. This method is used in a computer program to model the thermodynamic cycle of four-stroke spark ignition internal combustion engines. The method considers the effect of the fuel in the air-fuel-burned gas unburned gas mixture, air-fuel-burned gas unburned gas mixture equivalence ratio, temperature and pressure of the air-fuel-burned gas unburned gas mixture, burned gas mole fraction in the unburned gas, turbulence in the unburned gas and geometry of the combustion chamber. The results of the program for the laminar flame speed, turbulent flame speed and mass burning rate in an engine cycle are presented for a four-stroke spark ignition internal combustion engine.

Keywords: mass burning rate, flame speed, spark ignition, internal combustion engine.

INTRODUCTION

The mass burning rate of the unburned air-fuel-burned gas mixture inside the combustion chamber of an engine is equal to the product of the density of the unburned gas by the flame speed of the unburned gas by the surface area of the flame front. All these three quantities change with time during the engine cycle. Here we present a method to calculate these three quantities and consequently the mass burning rate at any time in the engine cycle during the combustion process. The density of the unburned gas is calculated using the ideal gas law from the temperature, pressure and molar mass of the unburned gas mixture. To calculate the flame speed in an instant of time in the engine cycle during the combustion phase we start to calculate the laminar flame speed of the air-fuel mixture for the fuel in the mixture, for the equivalence ratio of the air-fuel mixture and for a reference temperature and a reference pressure. Then we calculate the flame speed for the temperature and pressure of the unburned air-fuel gas mixture. Afterwards we calculate the effect on the flame speed of the burned gas mole fraction in the air-fuel-burned gas unburned gas mixture (Heywood, 1988). Following we take into account the effect of turbulence to calculate the turbulent flame speed of the unburned air-fuel- burned gas unburned gas mixture (Turns, 2012). At each instant of time we calculate two turbulent flame speeds. The first is the turbulent flame speed when the flame accelerates from laminar to fully developed turbulent flame speed. The second is the fully developed turbulent flame speed. For each instant of time we consider as the turbulent flame speed the lower of the two. The model is applied to model the combustion in one cylinder of a Peugeot TU3JP-KFW engine. This engine is a four cylinder, multipoint port fuel injection, with one intake valve, one exhaust valve and one spark plug per cylinder and satisfies the

Euro IV emissions standard. This method is used in a computer program to model the thermodynamic cycle of four-stroke spark ignition internal combustion engines (Carvalheira, 2016).

LAMINAR FLAME SPEED

The model presented here considers finite duration combustion. The laminar flame speed of air-fuel mixtures for an initial reference temperature T_0 and an initial reference pressure p_0, $S_{L,0}$, is given by Eq. (1) (Heywood, 1988) as a function of the air-fuel mixture equivalence ratio, ϕ, where B_m is the maximum laminar flame speed at reference temperature and pressure, B_ϕ is the quadratic coefficient for laminar flame speed at reference temperature and pressure and ϕ_m is the air-fuel mixture equivalence ratio at maximum laminar flame speed at reference temperature and pressure.

$$S_{L,0} = B_m + B_\phi(\phi - \phi_m)^2 \tag{1}$$

Table 1 presents the values of B_m, B_ϕ and ϕ_m used in this work which were obtained by a least square fitting to the data for air-gasoline mixtures presented in Fig. 9.25 of (Heywood, 1988) for a reference temperature of 300 K and for a reference pressure of 101325 Pa.

Table 1 - Values of B_m, B_ϕ and ϕ_m for air-gasoline mixtures used in this work

B_m [m/s]	B_ϕ [m/s]	ϕ_m
0.3561	-1.415	1.13

The laminar flame speed of air-gasoline mixtures, S_L, for conditions of temperature and pressure of the unburned mixture different from the reference values of 300 K and 101325 Pa is given by Eq. (2) where T_u is the unburned air-fuel mixture temperature, p is the unburned air-fuel mixture pressure, α and β are constants for a given fuel, equivalence ratio and burned gas diluent fraction and are given respectively by Eq. (3) and Eq. (4) (Heywood, 1988).

$$S_L = S_{L,0}\left(\frac{T_u}{T_0}\right)^\alpha \left(\frac{p}{p_0}\right)^\beta \tag{2}$$

$$\alpha = 2.18 - 0.80(\phi - 1) \tag{3}$$

$$\beta = -0.16 - 0.22(\phi - 1) \tag{4}$$

The effect of the mole fraction of burned gas in the air-fuel-burned gas unburned gas mixture, $\tilde{x}_{b,u}$, in the laminar flame speed of air-gasoline mixtures is given by Eq. (5) (Heywood, 1988):

$$S_L(\tilde{x}_{b,u}) = S_L(\tilde{x}_{b,u} = 0)\left(1 - 2.06\tilde{x}_{b,u}^{0.77}\right) \tag{5}$$

TURBULENT FLAME SPEED

In the early stages of the flame development the flame starts to be laminar and as the flame develops the flame front begins to corrugate and gradually changes to the fully developed turbulent regime. To calculate the flame speed during this transition period from laminar to turbulent the following method was developed.

The turbulence intensity of the flow in the unburned air-fuel mixture, v'_{rms}, is given by Eq. (6) where $\bar{u}_i$ is the mean inlet gas speed given by Eq. (6), adapted from (Heywood, 1988), where ρ_u is the density of the air-fuel-burned gas unburned gas mixture inside the cylinder and ρ_i is the density of the unburned air-fuel-burned gas unburned gas mixture in the intake port.

$$v'_{\mathrm{rms}} = 0.056\bar{u}_i \left(\frac{\rho_u}{\rho_i}\right)^{1/3} \tag{6}$$

The unburned gas mixture density inside the cylinder is given by the ideal gas law as presented in Eq. (7) where p_c is the pressure in the cylinder, R_u is the universal gas constant, M_u is the molecular weight of the air-fuel-burned gas unburned gas mixture and T_u is the temperature of the unburned gas mixture.

$$\rho_u = \frac{p_c M_u}{R_u T_u} \tag{7}$$

The unburned gas mixture density in the intake port is given by the ideal gas law as presented in Eq. (8) where p_i is the pressure in the intake port and T_i is the temperature of the unburned gas mixture in the intake port.

$$\rho_i = \frac{p_i M_u}{R_u T_i} \tag{8}$$

The molecular weight of the air-fuel-burned gas unburned gas mixture M_u is given by Eq. (9) where $\tilde{x}_f$ is the mole fraction of the fuel, $\tilde{x}_{\mathrm{O_2}}$ is the mole fraction of $\mathrm{O_2}$, $\tilde{x}_{\mathrm{N_2}}$ is the mole fraction of $\mathrm{N_2}$, $\tilde{x}_{b,u}$ is the mole fraction of burned gas in the air-fuel-burned gas unburned gas mixture, M_f is the molecular weight of the fuel, $M_{\mathrm{O_2}}$ is the molecular weight of $\mathrm{O_2}$, $M_{\mathrm{N_2}}$ is the molecular weight of $\mathrm{N_2}$ and M_b is the molecular weight of the burned gas mixture.

$$M_u = \tilde{x}_f M_f + \tilde{x}_{\mathrm{O_2}} M_{\mathrm{O_2}} + \tilde{x}_{\mathrm{N_2}} M_{\mathrm{N_2}} + \tilde{x}_{b,u} M_b \tag{9}$$

The mean inlet gas speed, $\bar{u}_i$, is given by Eq. (10) (Heywood, 1988) where η_v is the volumetric efficiency, A_c is the cross sectional area of the cylinder normal to the cylinder axis, A_{IV} is the maximum open area of the inlet valve and $\bar{S}_p$ is the mean piston speed.

$$\bar{u}_i = \eta_v \left(\frac{A_c}{A_{\mathrm{IV}}}\right) \bar{S}_p \tag{10}$$

The integral scale of turbulence in the unburned gas mixture inside the cylinder, l_0, is given by Eq. (11), adapted from (Heywood, 1988), where $L_{\mathrm{IV,max}}$ is the maximum lift of the intake valve, ρ_i is the density of the air-fuel-burned gas unburned gas mixture in the intake port and ρ_u is the density of the air-fuel-burned gas unburned gas mixture inside the cylinder.

$$l_0 = 0.80 L_{\mathrm{IV,max}} \left(\frac{\rho_i}{\rho_u}\right)^{1/3} \tag{11}$$

The Kolmogorov scale of turbulence is given by Eq. (12) (Heywood, 1988) where Re_{l_o} is the integral scale turbulence Reynolds number and is given by Eq. (13) (Heywood, 1988) where ν is the kinematic viscosity of the air-fuel-burned gas unburned gas mixture and v'_{rms} is the root mean square of the fluctuating velocity also called turbulence intensity of the flow in the air-fuel-burned gas unburned gas mixture.

$$l_k = l_0 \mathrm{Re}_{l_0}^{-3/4} \tag{12}$$

$$\mathrm{Re}_{l_0} = \frac{v'_{\mathrm{rms}} l_0}{\nu} \tag{13}$$

To calculate the acceleration of the flame speed a variable n_{lk} is defined for a certain time instant t by Eq. (14) which is the number of Kolmogorov length scales the flame has travelled since its ignition. In Eq. (14) t_{TI} is the ignition timing instant, $S_L(\tilde{x}_{b,u}, t)$ is the laminar flame speed of the air-fuel-burned gas unburned mixture with burned gas mole fraction $\tilde{x}_{b,u}$ at time instant t, $l_k(t)$ is the Kolmogorov length scale of the flow at time instant t.

$$n_{lk}(t) = \int_{t_{\mathrm{TI}}}^{t} \frac{S_L(\tilde{x}_{b,u}, t)}{l_k(t)} dt \tag{14}$$

The flame speed, S_b, at a given time t when it is accelerating from laminar to fully developed turbulent regime is given by Eq. (15) where k_{LT} is the constant of acceleration of the laminar flame to turbulent flame. This constant is equal to the increase in the area of the laminar flame front due to flame front corrugation when it travels a length equal to the Kolmogorov scale. The value of k_{LT} considered is given by Eq. (16).

$$S_b(t) = n_{lk}(t) \times k_{LT} \times S_L(\tilde{x}_{b,u}, t) \tag{15}$$

$$k_{LT} = \frac{1}{2}\left(1 + \frac{\pi}{2}\right) = 1.2854 \tag{16}$$

The flame speed, S_b, in fully developed turbulent regime is given by the Klimov equation, Eq (17) (Turns, 2012), where the effect of turbulence in the turbulent flame speed, is taken into account through v'_{rms}.

$$S_b(t) = S_L(\tilde{x}_{b,u}, t) \times 3.5 \left(\frac{v'_{\mathrm{rms}}(t)}{S_L(\tilde{x}_{b,u}, t)}\right)^{0.7} \tag{17}$$

In each instant of time t after the ignition timing the flame speed is evaluated through Eq. (15) and through Eq. (17). The value for the flame speed that is retained is the minimum value between these two values as given by Eq. (18). Physically what happens is that in the early stages of the flame development the flame starts to be laminar and as the flame develops the flame front begins to corrugate and the flame speed increases until it reaches the value for fully developed turbulent flame. In this phase the correct value for the flame speed is given by Eq. (15). After the value for fully developed turbulent flame has been attained, Eq. (15) will give a value for the flame speed that is larger than the value for the flame speed for fully developed turbulent flame, what is physically unrealistic and in this phase the correct value for the flame speed is given by Eq. (17).

$$S_b(t) = \min\left(n_{lk}(t) \times k_{LT} \times S_L(\tilde{x}_{b,u}, t), S_L(\tilde{x}_{b,u}, t) \times 3.5 \left(\frac{v'_{\mathrm{rms}}(t)}{S_L(\tilde{x}_{b,u}, t)}\right)^{0.7}\right) \tag{18}$$

MASS BURNING RATE

The mass burning rate is given by Eq. (19) where ρ_u is the unburned gas mixture density, S_b is the turbulent flame speed and A_b is the spherical burning area which is the area of the spherical surface within the combustion chamber which contains all the burned gases behind it.

$$\frac{dm_b}{dt} = \rho_u A_b S_b \tag{19}$$

The spherical burning area is given by Eq. (20) where V_b is the burned gas volume in the combustion chamber and r_b is the burned gas radius which is the radius of the spherical surface within the combustion chamber that contains all the burned gas behind it.

$$A_b = \frac{\partial V_b}{\partial r_b} \tag{20}$$

To determine this derivative a plot is made of the combustion chamber burned gas volume when the piston is on Top Dead Venter (TDC), $V_{b,\mathrm{TDC}}$, divided by the clearance volume, the combustion chamber volume when the piston is on TDC, V_c, as a function of the ratio of the burned gas radius, r_b, to the cylinder bore, B, for the combustion chamber of the engine and where the centre of the burned gas spherical surface is in the point where the middle plane between the spark plug electrodes intercepts the spark plug central electrode axis. The measurements of $V_{b,\mathrm{TDC}}$, for given values of r_b are made in a CAD 3D model of the combustion chamber of the engine when the piston is on TDC. Then a polynomial of fourth degree is fit to the data obtained for the combustion chamber burned gas volume divided by the clearance volume as a function of the ratio of the burned gas radius to the cylinder bore. The polynomial is presented in Eq. (21).

$$\frac{V_{b,\mathrm{TDC}}}{V_c} = a_4\left(\frac{r_b}{B}\right)^4 + a_3\left(\frac{r_b}{B}\right)^3 + a_2\left(\frac{r_b}{B}\right)^2 + a_1\left(\frac{r_b}{B}\right)^1 + a_o \tag{21}$$

Since the piston is close to TDC during the combustion process we assume that the burned gas volume fraction for a given burned gas radius during the combustion process is equal to the burned gas volume fraction for the same burned gas radius when the piston is on TDC, as expressed by Eq. (22).

$$\frac{V_b}{V}\left(\frac{r_b}{B}\right) = \frac{V_{b,\mathrm{TDC}}}{V_c}\left(\frac{r_b}{B}\right) \tag{22}$$

In consequence, for a given burned gas radius, r_b, during the combustion process the burned gas volume, V_b, is given by Eq. (23) were V is the instantaneous cylinder volume.

$$V_b = V\frac{V_{b,\mathrm{TDC}}}{V_c}\left(\frac{r_b}{B}\right) \tag{23}$$

Once calculated V_b for each r_b the spherical burning area of the flame front, A_b, is calculated by Eq. (20) where the derivative is calculated numerically.

Figure 1 presents the combustion chamber of Peugeot TU3JP-KFW engine at TDC. This combustion chamber has one intake valve, one exhaust valve and one spark plug. Figure 2 presents the burned gas volume of the combustion chamber of Peugeot TU3JP-KFW engine at TDC for a burned gas radius equal to 0.50 B. Figure 3. presents the plot of the combustion chamber burned gas volume when the piston is on TDC, $V_{b,\mathrm{TDC}}$, divided by the clearance

volume, V_c, as a function of the ratio of the burned gas radius, r_b, to the cylinder bore, B, and the polynomial fit for the combustion chamber of Peugeot TU3JP-KFW engine.

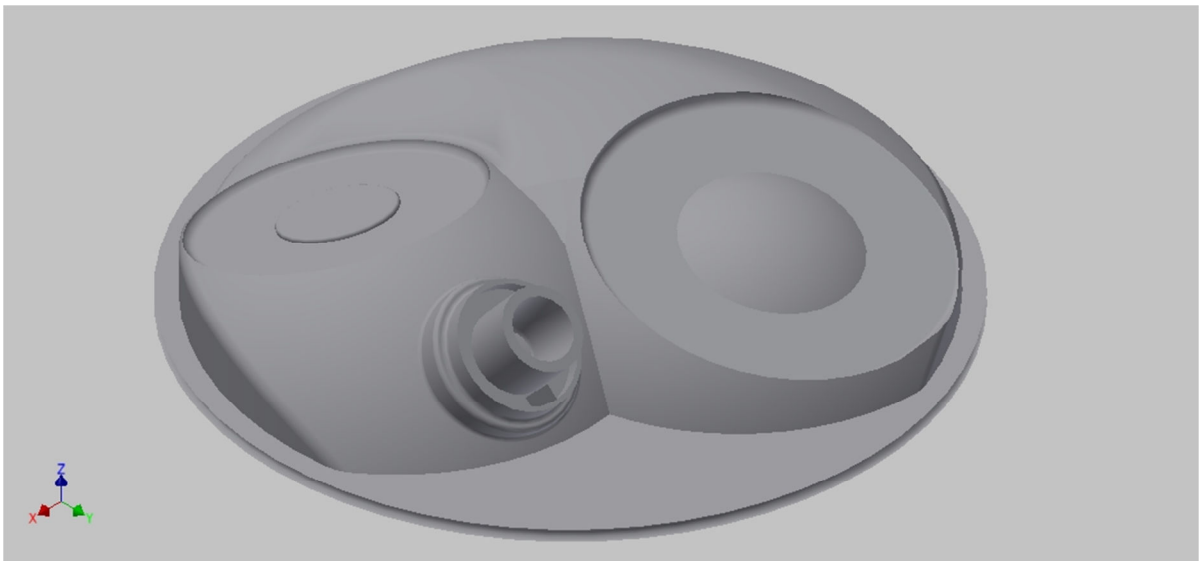

Fig. 1 - Combustion chamber of Peugeot TU3JP-KFW engine at TDC. This combustion chamber has one intake valve, one exhaust valve and one spark plug.

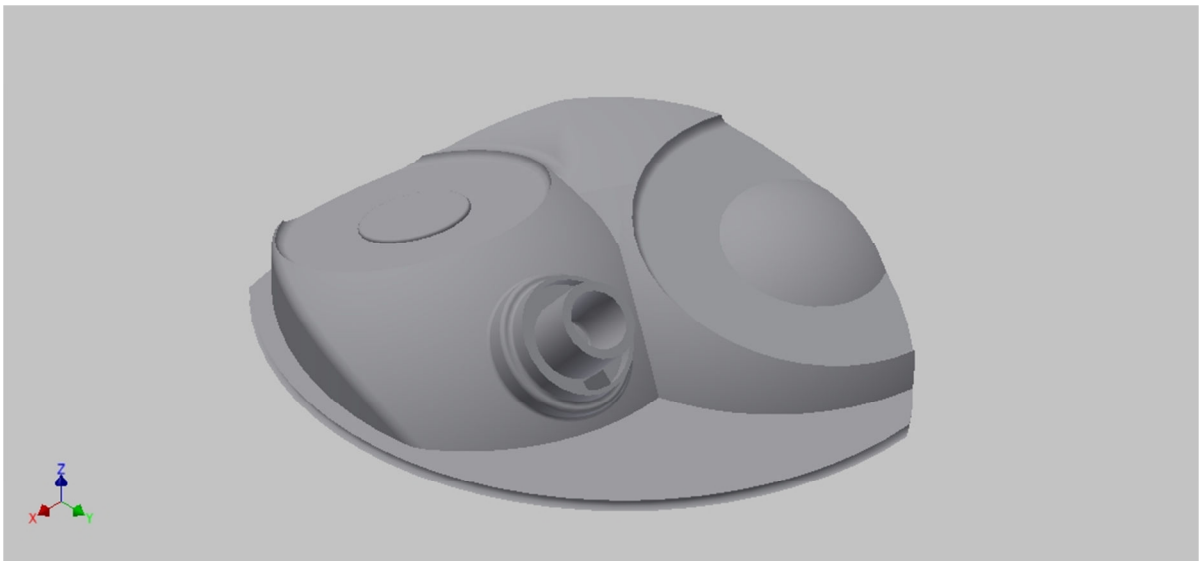

Fig. 2 - Burned gas volume of the combustion chamber of Peugeot TU3JP-KFW engine at TDC for a burned gas radius equal to 0.50 B.

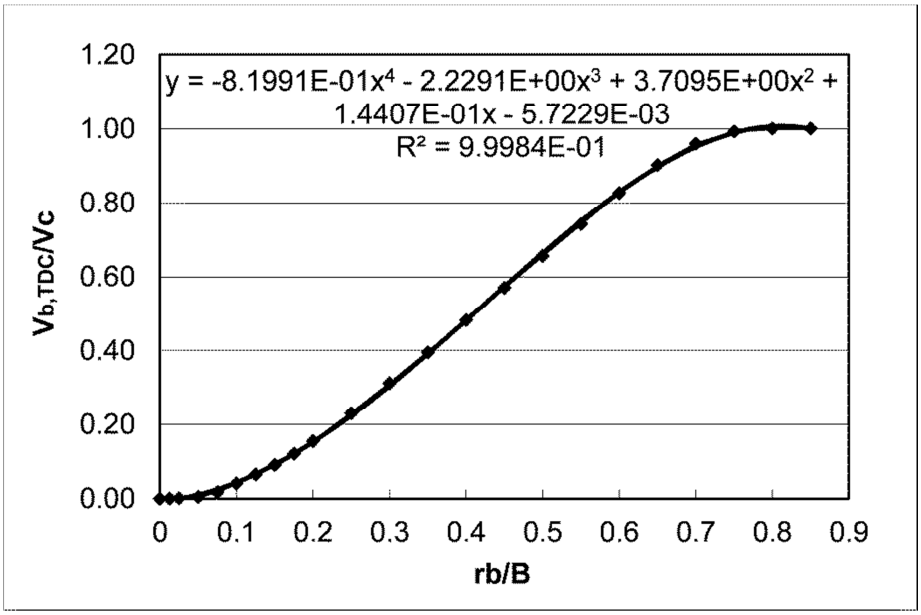

Fig. 3 - Combustion chamber burned gas volume when the piston is on TDC, $V_{b,\mathrm{TDC}}$, divided by the clearance volume, V_c, as a function of the ratio of the burned gas radius, r_b, to the cylinder bore, B, for the combustion chamber of Peugeot TU3JP-KFW engine.

Table 2 presents the coefficients of the polynomial of Eq. (21) and $(r_b/B)_{\max}$ for the combustion chamber of Peugeot TU3JP-KFW engine at TDC. In the first line are the values obtained from polynomial fitting to the geometrical data of the combustion chamber. In the second line are the values used in the simulation program. The values used in the simulation program were chosen in such a way that $V_{b,\mathrm{TDC}}/V_c$ was between 0 and 1.0 from $(r_b/B) = 0$ to $(r_b/B)_{\max}$. To avoid $V_{b,\mathrm{TDC}}/V_c$ to be negative when $(r_b/B) = 0$ or (r_b/B) is very small a_0 was made equal to zero. To avoid $V_{b,\mathrm{TDC}}/V_c$ to be larger than 1.0 $(r_b/B)_{\max}$ was made equal to 0.760.

Table 2 - Coefficients of the polynomial of Eq. (21) and $(r_b/B)_{\max}$ for the combustion chamber of Peugeot TU3JP-KFW engine at TDC. In the first line are the values obtained from polynomial fitting to the geometrical data of the combustion chamber. In the second line are the values used in the simulation program.

a_4	a_3	a_2	a_1	a_0	$(r_b/B)_{\max}$
-8.1991E-1	2.2291E0	3.7095E0	1.4407E-1	-5.7229E-3	0.800
-8.1991E-1	2.2291E0	3.7095E0	1.4407E-1	0	0.760

The mean expansion speed of the burned gas, u_b, is given by Eq. (24) (Heywood, 1988). This speed is the instantaneous mean speed of the burned gas front relative to a referential fixed to the engine combustion chamber. The volume fraction of the burned gases, y_b, is given by Eq. (25) where V_b is the burned gas volume, V_u is the unburned gas volume and V is the cylinder volume.

$$u_b = S_b \left(\frac{\rho_u}{\rho_b} (1 - y_b) + y_b \right) \tag{24}$$

$$y_b = \frac{V_b}{V} = \frac{V_b}{V_u + V_b} \tag{25}$$

Because it is difficult to evaluate precisely the value of y_b by Eq. (25) and because the combustion process develops when the piston is close to TDC, for the evaluation of y_b an approximation is made and y_b is calculated for a given r_b through Eq. (26) by using the polynomial of Eq. (21).

$$y_b = \frac{V_b}{V}\left(\frac{r_b}{B}\right) = \frac{V_{b,\mathrm{TDC}}}{V_c}\left(\frac{r_b}{B}\right) \tag{26}$$

The polynomial of Eq. (21) is valid for $r_b < r_{b,\max}$ where $r_{b,\max}$ is the maximum radius of the burned gas for a given combustion chamber geometry. After r_b attaining $r_{b,\max}$ the maximum possible value of V_b has been attained and y_b becomes equal to 1.0. The value of r_b for each instant of time is given by Eq. (27) where TI is the ignition timing.

$$r_b(t) = \int_{\mathrm{TI}}^{t} u_b(t)dt \tag{27}$$

RESULTS

Figures 4 and 5 present results for Peugeot TU3JP-KFW engine operating at 5500 rpm, at wide open throttle (WOT), with maximum brake torque (MBT) ignition timing, with $\phi = 1.0$, 298.15 K ambient temperature, 99000 Pa ambient pressure and dry air.

Figure 4(a) presents the results of the evolution of the calculated spherical burning area with crank angle. The spherical burning area presents a smooth evolution with the crank angle between the ignition timing (TI) and the end of combustion. It increases from the TI until 343º CA and then decreases until the end of the combustion process. Figure 4(b) presents the results of the evolution of the density of the unburned gas and of the density of the burned gas with crank angle. The density of the unburned gas presents a smooth evolution with the crank angle between the ignition timing (TI) and the end of combustion. It increases from the TI until 373º CA and then decreases until the end of the combustion process. The density of the burned gas presents a smooth evolution with the crank angle between the ignition timing (TI) and the end of combustion. It increases from the TI until 373º CA and then decreases until the end of the combustion process.

Figure 5(a) presents the results of the evolution of the laminar flame speed, $S_L(\tilde{x}_{b,u})$, of the turbulent flame speed, S_b, for the air-fuel-residual gas mixture and of the mean expansion speed of the burned gas, u_b, with the crank angle (CA). The laminar flame speed presents a smooth evolution with the crank angle between the ignition timing (TI) and the end of combustion. It increases from the TI until 352º CA and then decreases until the end of the combustion process. For the evolution of the turbulent flame speed with crank angle we observe two phases, one first phase, from 326º CA to 330º CA where the flame speed increases very rapidly, which corresponds to the acceleration of the flame from laminar to

fully developed turbulent and a second phase, where the flame speed increases more slowly from 330º CA to 368º CA and then decreases slowly from 368º CA until the end of the combustion process, which corresponds to the fully developed turbulent flame. For the evolution of the mean expansion speed of the burned gas with crank angle we observe two phases, one first phase where mean expansion speed of the burned gas increases very rapidly, from 326º CA to 330º CA, which corresponds to the acceleration of the flame from laminar to fully developed turbulent and a second phase where the mean expansion speed of the burned gas initially increases slightly and then slowly decreases until end of the combustion process which corresponds to the fully developed turbulent flame. Figure 5(b) presents the results of the evolution of the mass burning rate with the crank angle. The mass burning rate increases smoothly from 0 at TI to a maximum value at about 363º CA and then decreases to a finite value at the end of the combustion process at about 379º CA. We conclude from these results that the ratio of the turbulence intensity to the laminar flame speed, the temperature and density of the unburned gas and the flame front area have the major influence on the mass burning rate.

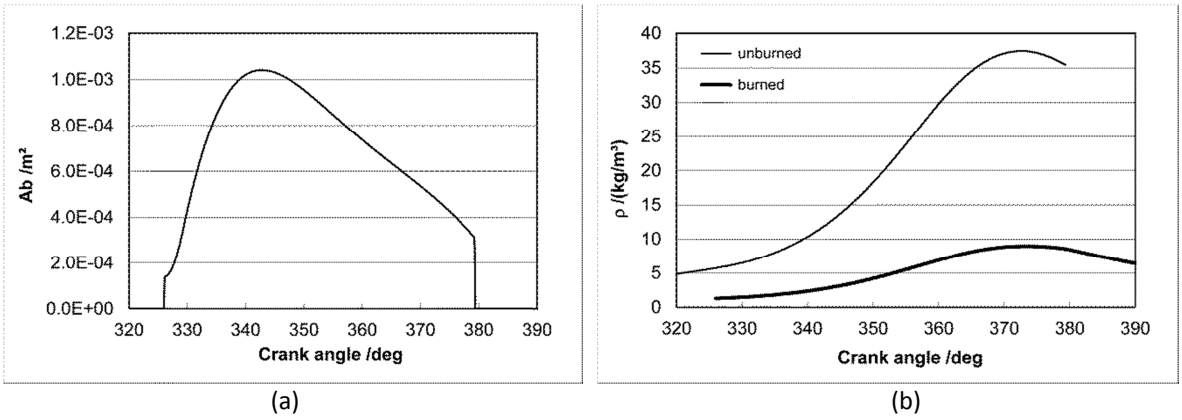

Fig. 4 - (a) Evolution of calculated spherical burning area with crank angle. (b) Evolution of the density of the unburned gas and of the burned gas with crank angle. Results for Peugeot TU3JP-KFW engine operating at 5500 rpm, at WOT, with MBT ignition timing, with $\phi = 1.0$, 298.15 K ambient temperature, 99000 Pa ambient pressure and dry air.

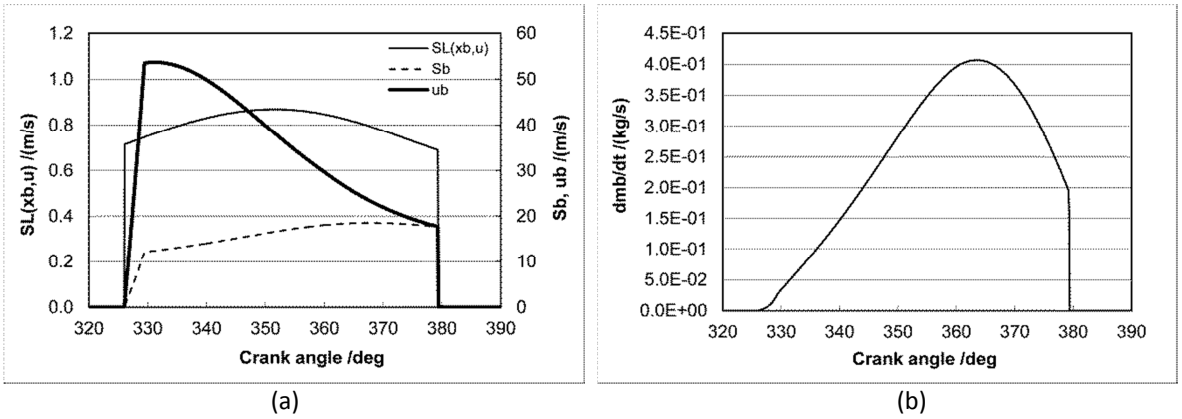

Fig. 5 - (a) Evolution of calculated laminar flame speed, turbulent flame speed and mean expansion speed of the burned gas with crank angle. (b) Evolution of calculated mass burning rate with crank angle. Results for Peugeot TU3JP-KFW engine operating at 5500 rpm, at WOT, with MBT ignition timing, with $\phi = 1.0$, 298.15 K ambient temperature, 99000 Pa ambient pressure and dry air.

Figure 6(a) presents experimental and simulation results obtained for Peugeot TU3JP-KFW engine operating at wide open throttle in the engine rotational speed range 800-6400 rpm. The experimental results were obtained by the Rototest Research Institute (Rototest Research Institute, 2000) and were performed in a roller test bench in the tractive wheels of a Peugeot 208 equipped with this engine. The experimental results were corrected for temperature equal to 298.15 K and 99000 Pa ambient pressure and dry air (ISO 1585 (5/82)). To obtain the results in the engine an estimative was made of the transmission efficiency. The simulation results were obtained with the simulation program with the engine operating with MBT ignition timing, with $\phi = 1.0$, 298.15 K ambient temperature, 99000 Pa ambient pressure and dry air. The agreement between the experimental and simulation results is good for 1500, 2000 and 5500 rpm. Between 2500 and 5000 rpm the brake torque and brake power obtained by experimental measurement is larger than the obtained by simulation and the maximum difference between the two is about 10 %. Between 6000 and 6400 rpm the brake torque and brake power obtained by simulation is larger than the obtained by experimental measurement and the maximum difference between the two is about 10 %.

Figure 6(b) presents experimental and simulation results for brake specific fuel consumption (bsfc) as a function of brake medium effective pressure (bmep) obtained for Peugeot TU3JP-KFW engine operating at part load at 3000 rpm engine rotational speed. The experimental results were obtained by (Prieur and Tilagone, 2006) in an engine test bench. The simulation results were obtained with the simulation program with the engine operating with MBT ignition timing, with $\phi = 1.0$, 298.15 K ambient temperature, 99000 Pa ambient pressure and dry air. For a given bmep the bsfc obtained by simulation is always larger than the obtained by experimental measurement. The agreement between the simulation and experimental results improves as bmep increases. In the 800-1040 kPa range the difference between the simulation and experimental results is about 8 % and at 300 kPa is about 20 %.

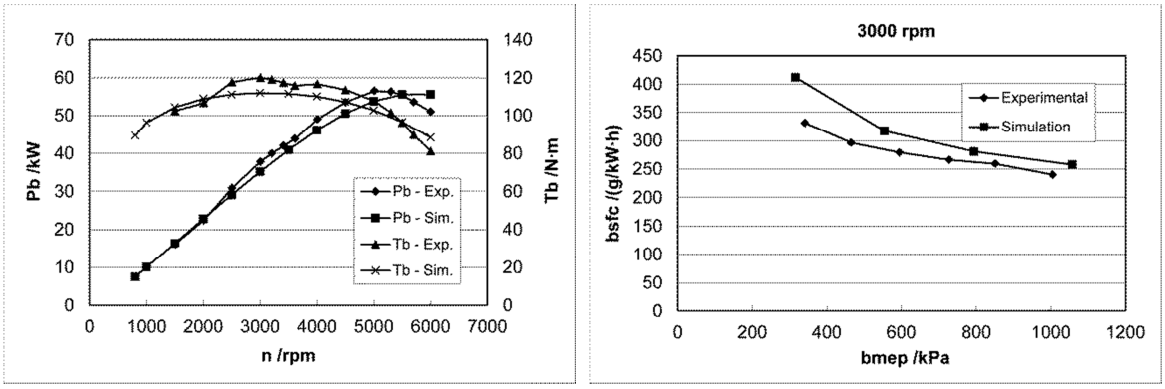

(a) (b)

Fig. 6 - Experimental results and simulation results obtained with the program for Peugeot TU3JP-KFW operating with MBT ignition timing, with $\phi = 1.0$, 298.15 K ambient temperature, 99000 Pa ambient pressure and dry air. (a) at wide open throttle operating in the range 800-6400 rpm. (b) at part load at 3000 rpm.

CONCLUSIONS

A method was presented for the calculation of mass burning rate in the combustion chamber of four-stroke spark ignition internal combustion engines. This method takes into account the effect on the mass burning rate of the fuel in the air-fuel-burned gas unburned gas mixture, the equivalence ratio of the air-fuel-burned gas unburned gas mixture, the temperature and pressure of the unburned gas mixture, the mole fraction of burned gas in the unburned gas

mixture, the ratio of the turbulence intensity to the laminar flame speed, the density of the unburned gas mixture and the evolution of the spherical burning area with the burned gas radius.

The results of the program for the laminar flame speed, turbulent flame speed, mean expansion speed of the burned gas and mass burning rate in an engine cycle were presented for a four-stroke spark ignition internal combustion engine.

We conclude from this study that the ratio of the turbulence intensity to the laminar flame speed, the temperature and density of the unburned gas and the spherical burning area have the major influence on the mass burning rate.

This method was used in a computer program to model the thermodynamic cycle of a four-stroke spark ignition internal combustion engine. The results for torque and power at WOT of the simulation program in the 800-6400 rpm engine rotational speed range were presented and compared with experimental results available in the literature for Peugeot TU3JP-KFW engine. The results for bsfc as a function of bmep of the simulation program at part load at 3000 rpm engine rotational speed were compared with experimental results available in the literature for Peugeot TU3JP-KFW engine.

ACKNOWLEDGMENTS

The author gratefully acknowledges the assignment of the Peugeot TU3JP-KFW engine by Automóveis do Mondego, Lda, to carry out this study.

REFERENCES

[1] Carvalheira, P. A Thermodynamic Cycle Model of Four-Stroke Spark Ignition Internal Combustion Engine. Symposium for Combustion Control 2016, Aachen, pp. 101-108, 2016.

[2] Heywood JB. Internal Combustion Engine Fundamentals. McGraw-Hill, New York, 1988, pp. 371-490.

[3] Turns, SR. An Introduction to Combustion: Concepts and Applications. 3rd Ed., McGraw-Hill, New York, 2012, pp. 427-485.

[4] Rototest Research Institute. Rototest Certificate of Performance STR-00111401, Peugeot 206 1.4. www.rototest.com/rri, Rönninge, 2000.

[5] Prieur A, Tilagone R, Le GNV: quel potentiel? Rapport, Institut Français du Pétrole, Rueil-Malmaison, 2006.